The American Journal of Pathology, Vol. 184, No. 5, May 2014

The American Journal of
PATHOLOGY
ajp.amjpathol.org

BIOMARKERS, GENOMICS, PROTEOMICS, AND GENE REGULATION

# Quantitatively Controlling Expression of miR-17∼92 Determines Colon Tumor Progression in a Mouse Tumor Model

Hong Jiang,*†‡§ Ping Wang,¶ Qilong Wang,† Baomei Wang,† Jingyao Mu,† Xiaoying Zhuang,† Lifeng Zhang,† Jun Yan,† Donald Miller,† and Huang-Ge Zhang*†‡

*From the Louisville Veterans Administration Medical Center,* Louisville, Kentucky; the James Brown Cancer Center† and the Department of Microbiology and Immunology,‡ University of Louisville, Louisville, Kentucky; the Department of General Surgery,§ the First Affiliated Hospital of Nanjing Medical University, Nanjing, China; and the State Key Laboratory of Virology,¶ Wuhan Institute of Virology, Chinese Academy of Sciences, Wuhan, China*

Accepted for publication January 23, 2014.

Address correspondences to Huang-Ge Zhang, Ph.D., Brown Cancer Center, University of Louisville, CTRB 309, 505 Hancock St., Louisville, KY 40202; or Hong Jiang, Ph.D., James Graham Brown Cancer Center, University of Louisville, CTRB 333, 505 Hancock St., Louisville, KY 40202. E-mail: h0zhan17@louisville.edu or h0jian03@louisville.edu.

The miRNA cluster miR-17∼92 targets mRNAs involved in distinct pathways that either promote or inhibit tumor progression. However, the cellular and molecular mechanisms underlying miR-17∼92 cluster-mediated protumorigenic or anti-tumorigenic effects have not been studied. Herein, we determined that inhibition of colon cancer progression is dictated by quantitatively controlling expression of the miR-17∼92 cluster. miR-19 in the context of the miR-17∼92 cluster at medium levels promoted tumor metastasis through induction of Wnt/β-catenin–mediated epithelial-mesenchymal transition by targeting to the tumor-suppressor gene, *PTEN*. However, higher levels of the miR-17∼92 cluster switched from *PTEN* to oncogenes, including *Ctnnb1* (β-catenin) via miR-18a, which resulted in inhibition of tumor growth and metastasis. However, overexpression of *Ctnnb1*in tumor cells with high-level miR-17∼92 did not lead to an increase in the levels of β-catenin protein, suggesting that other factors regulated by higher levels of miR-17∼92 might also contribute to inhibition of tumor growth and metastasis. Those unidentified factors may negatively regulate the production of β-catenin protein. Collectively, the data presented in this study revealed that higher levels of miR-17∼92 were a critical negative regulator for activation of the Wnt/β-catenin pathway and could have a potential therapeutic application. *(Am J Pathol 2014, 184: 1355–1368; http://dx.doi.org/10.1016/j.ajpath.2014.01.037)*

miRNAs are snRNAs that are processed from primary transcripts by double-stranded RNA–specific endonucleases (Drosha and Dicer).[1,2] miRNAs are known to negatively regulate gene expression mainly by directly binding with 3′-untranslated regions (3′-UTRs) of their target genes.[3] Studies have shown that miRNAs are implicated in cancer progress, including colorectal cancer.[4,5] Many miRNAs have been demonstrated to contribute to cancer progress through modulating different targets.[6–8]

The miR-17∼92 cluster produces a single polycistronic primary transcript processed to yield six individual mature miRNAs: miR-17, miR-18a, miR-19a, miR-19b, miR-20a, and miR-92a. The importance of miR-17∼92 overexpression in tumor initiation and progression is well documented by the observation that transgenic expression of this cluster in lymphocytes leads to a lymphoproliferative disorder in mice.[9] Furthermore, data published recently suggest that each of the six constituent members of miR-17∼92 has a different role during tumor progression, and alteration in the balanced expression of individual miR-17∼92 members has a significant effect on tumor progression.[10–12] Previous observations overwhelmingly support a dominant role of *miR-19a* and *miR-19b* in promoting tumorigenesis[10,11] and in tumor angiogenesis.[13] However, there is also evidence that miR-

This work was supported by NIH grants UH2TR000875 (National Center for Advancing Translational Sciences), National Cancer Institute grants RO1CA13703 and RO1CA116092, the Louisville Veterans Administration Medical Center Merit Review grants, and Career Scientist Award (H.-G.Z.).

Disclosures: None declared.


http://dx.doi.org/10.1016/j.ajpath.2014.01.037

17∼92 may function in tumor suppression through targeting *AIB1*, *IL-8*, and *Cyclin D1*, by inhibiting cellular invasion, tumor metastasis, and proliferation.[14] Loss of heterozygosity at *13q12-q13*, which is the locus of the *miR-17-92* cluster, is associated with multiple tumor progression and poor prognosis, including breast cancer,[15] squamous cell carcinoma of the larynx,[16] retinoblastoma,[17] and hepatocellular carcinoma.[18] By using a high-resolution, array-based, comparative genomic hybridization in human tumor specimens, the *miR-17-92* cluster was found being deleted in 16.5% of ovarian cancers, 21.9% of breast cancers, and 20.0% of melanoma.[19] The cellular and molecular mechanisms underlying the miR-17∼92 cluster that mediated protumorigenic or antitumorigenic effects is not fully understood. We hypothesize that expression levels of miRNAs may play an important regulatory role in tumor progression by acting as either a protumorigenic or an anti-tumorigenic molecule. Proving this hypothesis could have a great impact on the miRNA field in general because miRNAs are produced endogenously and have been identified as important regulators of gene expression in a wide range of organisms and biological systems.

Aberrant activation of Wnt/β-catenin signaling is involved in various cancers,[20,21] including human colorectal cancers.[22] Numerous studies have demonstrated that miRNAs are important regulators of the Wnt/β-catenin signaling pathway, including the *miR-200* family[23] and *miR-9*.[24] A few data recently published suggest that miR-17∼92 could also regulate osteogenesis[25] and cardiac[26] differentiation in *in vitro* models through interaction with the Wnt signaling pathway. However, to our knowledge, no data published suggest that miR-17∼92 directly targets β-catenin, the central downstream effector of the Wnt/β-catenin pathway.

In this study, we demonstrate that quantitatively controlling expression of the miR-17∼92 cluster determines whether the miR-17∼92 cluster is capable of being a tumor suppressor. We show that higher levels of miR-18a in the context of the miR-17∼92 cluster suppress the Wnt/β-catenin pathway by directly targeting β-catenin. Therefore, modulating levels of the *miIR-17∼92* cluster could have potential application in treatment of neoplastic disease.

## Materials and Methods

### Cell Lines and Plasmids

Mouse CT26, CMT-93, and MCA38 colon cancer cell lines were maintained in RPMI 1640 medium (Invitrogen, Carlsbad, CA), supplemented with 10% fetal bovine serum (Invitrogen), penicillin, and streptomycin (Invitrogen). The 4T1 mouse breast cancer cell line was maintained in Dulbecco's modified Eagle's medium (Invitrogen), supplemented with 10% fetal bovine serum, penicillin, and streptomycin. L-Wnt3a (CRL-2647; ATCC, Manassas, VA) and L-cells (CRL-2648; ATCC) were grown, and conditioned medium was generated according to instructions. All cell lines were obtained from ATCC. To generate cell lines stably expressing the miR-17∼92 cluster, mouse cancer cell lines were seeded into a 6-well plate and cultured overnight, and cells were then transfected with PIG-miR-Ctrl Vector or PIG-miR-17∼92 wild type (WT) [provided by Dr. Andrea Ventura (Memorial Sloan-Kettering Cancer Center, New York, NY)].[10] At 6 hours after transfection, cells were returned to regular culture media containing 7.5 g/mL puromycin (Sigma, St. Louis, MO) (CT26 cell line) or 5 g/mL puromycin (4T1 cell line). At 2 weeks after drug selection, green fluorescent protein−positive ($GFP^+$) cells were sorted using an FACSAria III Flow Cytometer (BD Biosciences, San Jose, CA) and were seeded into a 96-well plate for monoclonal selection by serial dilution. M51 Super 8x FOPFlash (TOPFlash mutant),[27] pTK-Slug,[28] MSCV-β-Catenin ΔGSK-KT3,[29] pcDNA-S33Y-β-catenin,[30] pGL3-Control-*PTEN*-3′UTR-WT, and pGL3-Control-*PTEN*-3′UTR-MUT[31] were purchased from Addgene (Cambridge, MA).

### Mouse Models

Female BALB/c mice were purchased from the Jackson Laboratory (Bar Harbor, ME). To generate mouse tumor models, $1 \times 10^5$ CT26 tumor cells per mouse were s.c. injected. Tumors were measured with a caliper, and tumor volumes were calculated using the formula length × $width^2$ and presented as means ± SD. To generate a mouse tumor metastasis model, $1 \times 10^6$ CT26 tumor cells per mouse were i.v. injected via tail vein. To generate a mouse model of breast cancer metastasis, $5 \times 10^5$ 4T1 tumor cells per mouse were injected into the mammalian fat pads. To generate a mouse model of colon cancer liver metastasis, $1 \times 10^6$ CT26 tumor cells per mouse were injected into the spleen, as previously described.[32] All animal studies were performed in accordance with protocols approved by the University of Louisville Institutional Animal Care and Use Committee (Louisville, KY).

### Microarray Profiling

Total RNA from miR-Ctrl, miR-17∼$92^{Med}$, and miR-17∼$92^{Hi}$ cells (three subclones of each group) was isolated and subsequently processed for microarray hybridization using Affymetrix (Santa Clara, CA). ExonExprChipMoGene Arrays were performed according to the manufacturer's instructions (Affymetrix). Raw data (three samples per cell line) were preprocessed by the robust multiarray analysis method, and differentially expressed genes were determined using the significance analysis of microarray algorithm. Target sets and significant microarray data were subjected to Ingenuity Pathway Analysis (Ingenuity Systems, Redwood City, CA).

### Plasmid Construction

To construct psiCHECK2-*Ctnnb1*-3′-UTR-WT, the XhoI-NotI 3′-UTR (*Ctnnb1*) fragment was PCR amplified from

mouse genomic DNA, which contained four miR-17∼92 binding sites, using the following primers: forward (XhoI), 5′-ATCTCGAGGGCCTGTAGAGTTGCTGAGAGGG-3′; and reverse (NotI), 5′-GCGCGGCCGCCGGTTCTTAGAAAT-3′. The PCR cycle consisted of an initial step of 95°C for 3 minutes, followed by 30 cycles of 95°C for 1 minute, 55°C for 50 seconds, and 72°C for 1 minute, and then followed by an elongation step of 72°C for 7 minutes. The WT *Ctnnb1* 3′-UTR was then inserted downstream from a *Renilla* luciferase reporter psiCHECK2 (XhoI and NotI sites are indicated; Promega, Madison, WI): *Ctnnb1*-3′-UTR-WT: (+296 ∼ +650 bp): AT*CTCGAG*(*Xho* I)GGCCTGTAGAGTTGCTGAGAGGGCTCGAGGGGTGGGCTGGTATCTCAGAAAGTGCCTGACACACTAACCAAGCTGAGTTTCCTATGGGAACAGTCGAAGTACGCTTTTTGTTCTGGTCCTTTTTGGTCGAGGAGTAACAATACAAATGGATTTGGGGAGTGACTCACGCAGTGAAGAATGCACACGAATGGATCACAAGATGGCGTTATCAAACCCTAGCCTTGCTTGTTCTTTGTTTTAATATCTGT*AGTGGTGCTGACTTTGCTTGCT*TTTATTTTTTGCAGTAACTGTTAGTTTTTAAGTAGTGTTATGTTCTAGTGAACCTGCTACAGCAATTTCTGATTTCTAAGAACCG*GCGGCCGC*(*Not* I)GC.

## Colony Formation Assay

Cells were starved for 24 hours before treatment. A total of $1 \times 10^3$ cells per well were seeded into 6-well cell culture plates and cultured for 2 weeks with complete cell culture medium (RPMI 1640 medium, supplemented with 10% fetal bovine serum). Colonies were fixed with 1:1 methanol/acetone, stained with crystal violet (Sigma). Cell colonies were visualized using a Nikon ECLIPSE TS100 inverted microscope (Nikon, Tokyo, Japan). The number of colonies was determined by counting colonies in five random fields from three wells for each treatment. All experiments were performed in triplicate.

## Cell Migration Assay

For the transwell migration assay, chambers were rehydrated overnight and a 100-μL suspension of $1 \times 10^5$ live cells in serum-free RPMI 1640 medium was added to 6.5-mm transwell, 8-μm polycarbonate membrane inserts (Corning Life Sciences, Corning, NY). They were placed in 24-well plates containing 500 μL of 10% fetal bovine serum−containing complete cell culture medium per well. The plates were incubated for 6 hours at 37°C. At the end of the incubation period, the number of migrating cells on the bottom was determined by counting cells in five random fields for each treatment using an Olympus IX71 inverted microscope (Olympus OpticalCo. Ltd, Tokyo, Japan), with a magnification of ×200.

## *In Vivo* Imaging of Tumor Metastasis

To monitor tumor cell metastasis *in vivo*, tumor cell lines were first labeled using a near-infrared lipophilic carbocyanine dye−dioctadecyl−tetramethylindotricarbocyanine iodide (DiR; Invitrogen). Cells were incubated with DiR dye ($1 \times 10^7$ cells in 10-mL PBS containing 3.5 μg/mL dye and 0.5% ethanol) for 30 minutes at 37°C.[33] Thereafter, cells were washed twice with PBS and the viability of labeled cells was verified by trypan blue staining. Each mouse received

**Table 1** List of Primers Used in the Study

| Gene | Forward primer | Reverse primer |
|---|---|---|
| *E2f1* | 5′-GCCCTTGACTATCACTTTGGTCTC-3′ | 5′-CCTTCCCATTTTGGTCTGCTC-3′ |
| *Bim* | 5′-CGACAGTCTCAGGAGGAACC-3′ | 5′-CCTTCTCCATACCAGACGGA-3′ |
| *p21* | 5′-GTGATTGCGATGCGCTCATG-3′ | 5′-TCTCTTGCAGAAGACCAATC-3′ |
| *Axin2* | 5′-GCCAATGGCCAAGTGTCTCT-3′ | 5′-GCGTCATCTCCTTGGGCA-3′ |
| *Klf4* | 5′-ATCTTTCTCCACGTTCGCGTCTG-3′ | 5′-AAGCACTGGGGGAAGTCGCTTC-3′ |
| *Tcf4* | 5′-CACAACGGAGCGATGGGTA-3′ | 5′-GGGTGGGTTCAAGTCAGG-3′ |
| *Egfr* | 5′-TTGGTGCCACCTGTGTGAA-3′ | 5′-TCGGACACATGAGCCATGAT-3′ |
| *c-Myc* | 5′-AAGGCCCCCAAGGTAGTGA-3′ | 5′-TGCTCGTCTGCTTGAATGGA-3′ |
| *Ccnd1* | 5′-TCCTCTCCAAAATGCCAGAG-3′ | 5′-GCAGGAGAGGAAGTTGTTGG-3′ |
| *Lef1* | 5′-GGAGCCCTACCACGACAA-3′ | 5′-CCACGGGCACTTTATTTGA-3′ |
| *Wnt3a* | 5′-CTGCACCACCGTCAGCAA-3′ | 5′-CCTGGCATCGGCAAACTC-3′ |
| *Ctnnb1* | 5′-CAAGTGGGTGGTATAGAGG-3′ | 5′-TCAATGGGAGAATAAAGCAGC-3′ |
| *Cdh1* | 5′-GTCTCCTCATGGCTTTGC-3′ | 5′-CTTTAGATGCCGCTTCAC-3′ |
| *Vim* | 5′-CCGCTTTGCCAACTACAT-3′ | 5′-TCTCTTGCAGAAGACCAATC-3′ |
| *Twist1* | 5′-AGCGGGTCATGGCTAACG-3′ | 5′-GGACCTGGTACAGGAAGTCGA-3′ |
| *Snai1* | 5′-GTCGTCCTTCTCGTCCACC-3′ | 5′-GGCCTGGCACTGGTATCTC-3′ |
| *Snai2* | 5′-TCCCATTAGTGACGAAGA-3′ | 5′-CCCAGGCTCACATATTCC-3′ |
| *Zeb1* | 5′-CCATACGAATGCCCGAACT-3′ | 5′-ACAACGGCTTGCACCACA-3′ |
| *Zeb2* | 5′-GAGCTTGACCACCGACTC-3′ | 5′-TTGCAGGACTGCCTTGAT-3′ |
| *Gapdh* | 5′-GTTGTCTCCTGCGACTTCA-3′ | 5′-GGTGGTCCAGGGTTTCTTA-3′ |
| *Actb* (β-Actin) | 5′-GATCTGGCACCACACCTTCT-3′ | 5′-GGGGTGTTGAAGGTCTCAAA-3′ |

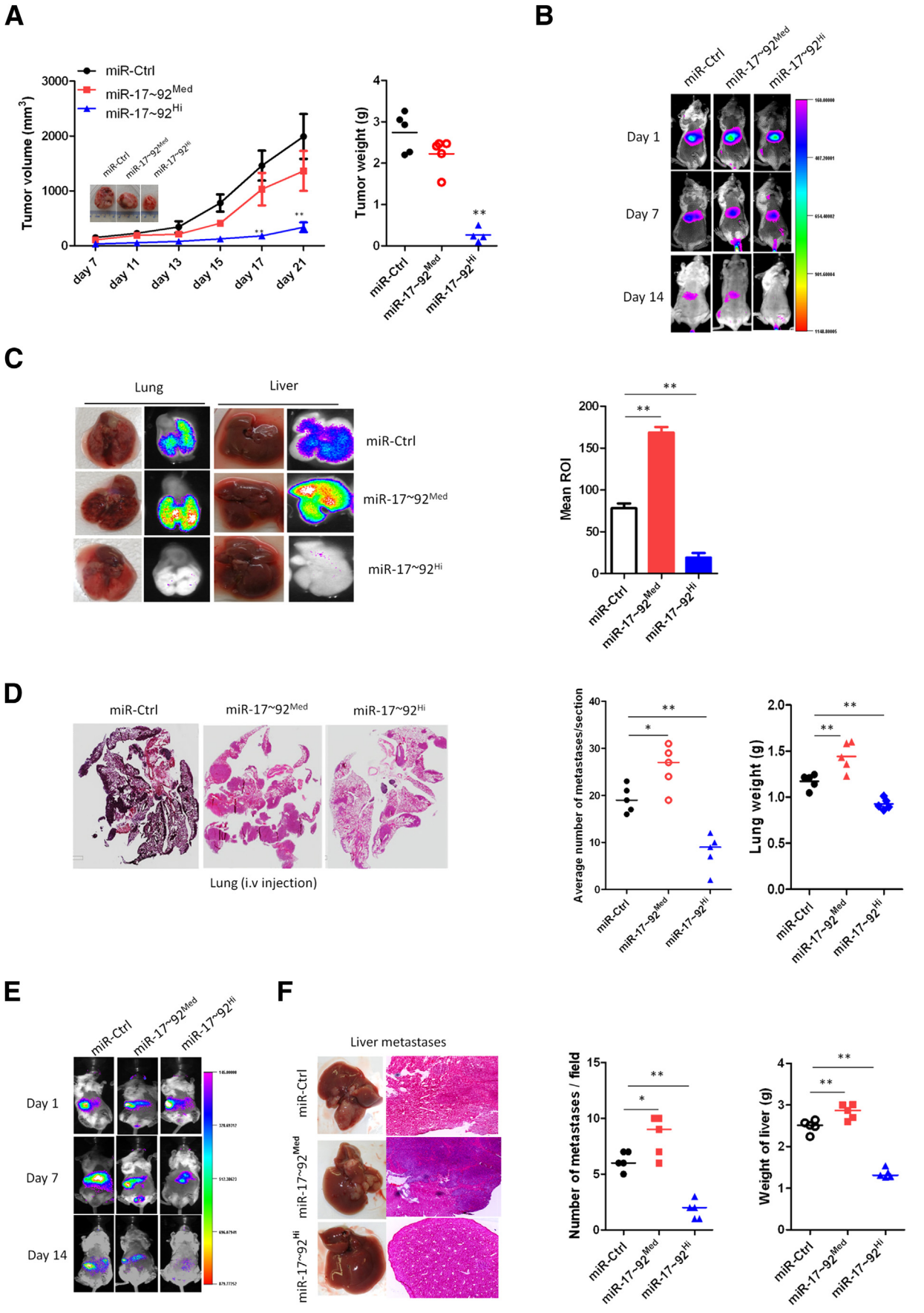
A
miR-Ctrl
miR-17~92Med
miR-17~92Hi
Tumor volume (mm3)
3000
2000
1000
0
day 7
day 11
day 13
day 15
day 17
day 21
Tumor weight (g)
4
3
2
1
0
**
miR-Ctrl
miR-17~92Med
miR-17~92Hi
B
miR-Ctrl
miR-17~92Med
miR-17~92Hi
Day 1
Day 7
Day 14
C
Lung
Liver
miR-Ctrl
miR-17~92Med
miR-17~92Hi
Mean ROI
200
150
100
50
0
**
**
miR-Ctrl
miR-17~92Med
miR-17~92Hi
D
miR-Ctrl
miR-17~92Med
miR-17~92Hi
Lung (i.v injection)
Average number of metastases/section
40
30
20
10
0
**
*
miR-Ctrl
miR-17~92Med
miR-17~92Hi
Lung weight (g)
2.0
1.5
1.0
0.5
0.0
**
**
miR-Ctrl
miR-17~92Med
miR-17~92Hi
E
miR-Ctrl
miR-17~92Med
miR-17~92Hi
Day 1
Day 7
Day 14
F
Liver metastases
miR-Ctrl
miR-17~92Med
miR-17~92Hi
Number of metastases / field
15
10
5
0
**
*
miR-Ctrl
miR-17~92Med
miR-17~92Hi
Weight of liver (g)
4
3
2
1
0
**
**
miR-Ctrl
miR-17~92Med
miR-17~92Hi

$1 \times 10^6$ DiR-labeled tumor cells administered i.v. via tail vein. Mice were then imaged at different time points using a Carestream Molecular Imaging System (Carestream Health, Woodbridge, CT).

## Real-Time PCR

Total RNA was isolated from tumor tissues or cells using an RNeasy Mini Kit (Qiagen, Frederick, MD). Quantitative real-time RT-PCR analysis of the mature miR-17∼92 cluster was performed using an miRNA-specific TaqMan MicroRNA Assay Kit (Applied Biosystems, Foster City, CA). Relative quantification of selected mRNA and pre-miR-17∼92 was performed using a CFX96 Realtime System (Bio-Rad Laboratories, Hercules, CA) and SsoFast Evagreen supermixture (Bio-Rad Laboratories), according to the manufacturer's instructions. All primers were obtained from Eurofins MWG Operon (Huntsville, AL). Expression values were normalized to murine glyceraldehyde-3-phosphate dehydrogenase (Gapdh) or β-actin. The sequences of the primers are listed in Table 1.

## Western Blot Analysis

Western blot analyses were done as previously described.[21,34] Cell lysates were harvested with 2% SDS-125 mmol/L Tris/HCl (pH 7.4) or for nondenaturing conditions using commercial cell lysis buffer (Cell Signaling Technology, Beverly, MA) supplemented with protease and phosphatase inhibitors (Roche, Indianapolis, IN). Cell lysates were resolved in Tris/glycine SDS/PAGE gels (Invitrogen) and transferred to polyvinylidene difluoride membranes (Invitrogen). Membranes were probed with primary antibodies overnight at 4°C. The primary antibodies were as follows: anti-Wnt3a, anti-Wnt5a, anti−p-Lrp6, anti-Lrp6, anti-Dvl2, anti-Tcf4, anti−β-catenin, anti−E-cadherin, anti-Akt (Ser473), anti−p-Akt, and anti-Axin1, all purchased from Cell Signaling; anti-PTEN, anti-GAPDH, and anti−β-actin were all purchased from Santa Cruz Biotechnology (Santa Cruz, CA). Membranes were developed with the Odyssey imager (LiCor Inc, Lincoln, NE). The signal intensity (Target: Gapdh, β-actin, or α-tubulin) for each band was determined using ImageJ software version 1.47 (NIH, Bethesda, MD).

## Luciferase Assays

A total of $5 \times 10^4$ CT26 cells were seeded into 24-well plates, cultured overnight, and the cells were then transfected with *Renilla* luciferase constructs, together with different doses of plasmids encoding mmu-pre-miR-17∼92 using Lipofectamine 2000 (Invitrogen). After 24 hours of incubation, cells were subjected to a Luciferase assay. *Renilla* luciferase activities were evaluated using the dual-luciferase reporter assay system (Promega). For the Topflash assay, $5 \times 10^4$ miR-Ctrl, miR-17∼92$^{Med}$, or miR-17∼92$^{Hi}$ cells were seeded into 24-well plates, cultured overnight, and cells were then transfected with T cell factor/lymphoid enhancer binding factor reporter Topflash [donated by David Piwnica-Worms (Washington University, St. Louis, MO)].[35] Luciferase activity was assayed 24 hours after treatment using the luciferase assay system, according to the manufacturer's protocol (Promega). The number of cells present in each sample was also counted to normalize the luciferase activity to the total number of cells.

## Immunohistochemistry

Immunohistochemistry was performed on formalin-fixed, paraffin-embedded tissues. Serial sections (4 μm thick) were stained with H&E for morphological analysis. For tissue immunofluorescent staining, slides were washed three times (5 minutes each) with PBST (PBS and 0.1% Tween 20). The tissue was permeabilized by incubating the slides in 1% Triton X-100 in PBS at 25°C for 15 minutes and then washed three times in PBST. After blocking for 1 hour at 25°C in blocking buffer (PBS containing 10% bovine serum albumin), slides were incubated overnight in a humidity chamber with anti-mouse antibodies. β-Catenin and E-cadherin monoclonal antibodies (BD Biosciences) were diluted 1:50 in blocking buffer. After another three PBST washes, slides were incubated with Alexa 594− or Alexa 647−conjugated goat anti-mouse secondary antibody at a 1:500 dilution (Molecular Probes, Grand Island, NY). Slides were then washed and nuclei were counterstained with DAPI. For cell immunofluorescent staining, cell lines were seeded into a chamber slide (Lab-Tek II Chamber Slide System; Thermo Fisher Scientific, Waltham, MA) and cultured overnight. Cells

**Figure 1** **A:** miR-17∼92 inhibits tumor growth and metastasis *in vivo*. Growth curves of control (miR-Ctrl), medium levels of miR-17∼92 cluster (miR-17∼92$^{Med}$), and high levels of miR-17∼92 cluster (miR-17∼92$^{Hi}$) tumors in BALB/c mice (five mice per group). The inner panel shows the morphological characteristics of tumors. The tumor weights from primary tumors ($n = 5$) from the same mice. miR-Ctrl, miR-17∼92$^{Med}$, and miR-17∼92$^{Hi}$ monoclonal cell lines were labeled with 1,1′-Dioctadecyl-3,3,3′,3′-Tetramethylindotricarbocyanine Iodide (DIR) dye. The DIR dye−labeled cells were then injected i.v. into 6-week-old female BALB/c mice. **B:** Tumor cell metastasis was monitored using a live imaging system by detecting the DIR fluorescence. **C:** The signals of the DIR-labeled tumor cells in the lung and liver. The histogram shows the mean intensity of the DIR fluorescence at 14 days after i.v. injection of miR-Ctrl, miR-17∼92$^{Med}$, or miR-17∼92$^{Hi}$ monoclonal cells in BALB/c mice. Mean intensity of region of interest = Sum Intensity/Area ($n = 5$). **D:** H&E staining of lung tumors from 14-day tumor-bearing mice that were i.v. injected with miR-Ctrl, miR-17∼92$^{Med}$, or miR-17∼92$^{Hi}$ monoclonal cells in BALB/c mice. The graphs show the number of metastatic sites per section and the mean lung weights, respectively. miR-Ctrl, miR-17∼92$^{Med}$, and miR-17∼92$^{Hi}$ monoclonal cell lines were labeled with DIR dye. DIR dye−labeled cells were then injected into the spleens of 6-week-old female BALB/c mice. **E:** Tumor cell metastasis was monitored using a live imaging system by detecting the DIR fluorescence; representative images from each group of tumor-bearing mice are shown. **F:** The morphological characteristics of miR-Ctrl, miR-17∼92$^{Med}$, and miR-17∼92$^{Hi}$ liver tumors and H&E staining of divided liver tissues from mice 14 days after splenic injection of miR-Ctrl, miR-17∼92$^{Med}$, or miR-17∼92$^{Hi}$ monoclonal cells in BALB/c mice. The graphs show the number of metastases per field and the mean liver weights, respectively. Error bars represent ±SD (two-way analysis of variance) in **A**, **left panel**; median value (one-way analysis of variance) in **A**, **right panel**, **D**, and **F**; and ±SD (one-way analysis of variance) in **B**. $^*P < 0.05$, $^{**}P < 0.01$.

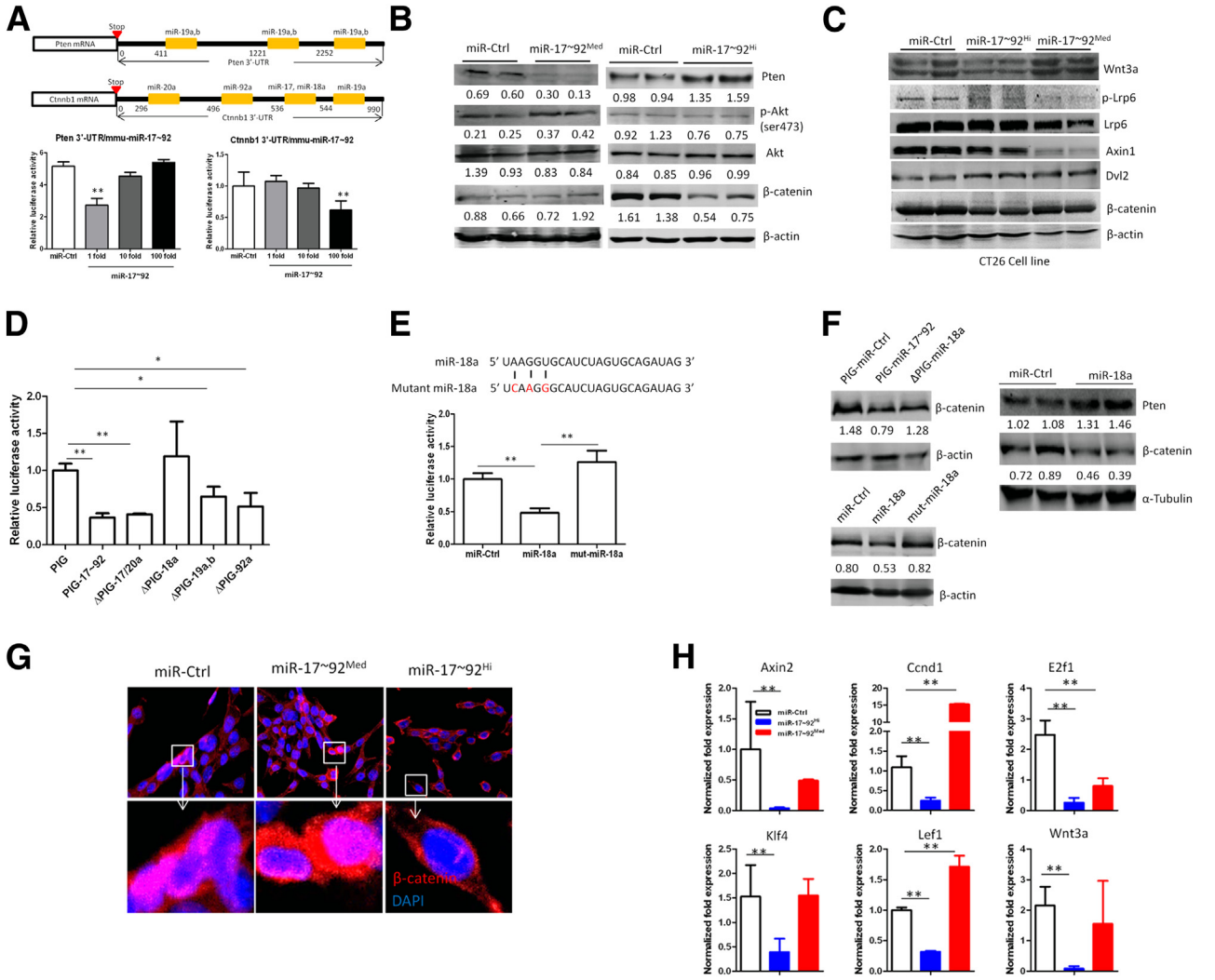


**Figure 2** Genome-wide target prediction of medium/high levels of miR-17∼92. **A:** Schematic representation of the 3′-UTR of murine *PTEN* and Ctnnb1. The 3′-UTR encoding miR-17∼92 binding sites were ligated downstream of the luciferase open reading frame. CT26 cells were cotransfected with pGL3-*PTEN* 3′-UTR-WT luciferase reporter plasmids or psiCHECK2-Ctnnb1 3′-UTR *Renilla* luciferase reporter plasmids, together with plasmids encoding mmu-miR-17∼92, as indicated. Luciferase activity was measured 24 hours after transfection. **B:** Western blot analysis shows the levels of proteins involved in the AKT/β-catenin pathway of miR-Ctrl and miR-17∼92$^{Med}$ cell lines. **C:** The intensity of each band was measured with ImageJ software version 1.47 and labeled below the bands. Western blot analysis shows the expression of proteins in the Wnt/β-catenin pathway in miR-Ctrl, miR-17∼92$^{Med}$, or miR-17∼92$^{Hi}$ cell lines. β-Actin was used as a loading control. CT26 cells were cotransfected with psiCHECK2-Ctnnb1 3′-UTR *Renilla* luciferase reporter plasmids, together with plasmids encoding mmu-miR-17∼92 (PIG-17∼92), mutant miR-17/20a (PIG-Δ17/20a), mutant miR-18a (PIG-Δ18a), mutant-miR-19a,b (PIG-Δ19a,b), and mutant-miR-92a (PIG-Δ92a), as indicated. **D:** *Renilla* luciferase activity 24 hours after transfection. **E:** Scheme shows the mutant sites of miR-18a. CT26 cells were cotransfected with psiCHECK2-Ctnnb1 3′-UTR *Renilla* luciferase reporter plasmids, together with miR-18a mimic or mutant miR-18a, as indicated. *Renilla* luciferase activity 24 hours after transfection. **F:** Western blot analysis shows the expression of β-catenin or *PTEN* proteins in CT26 cells 48 hours after transfection with plasmids encoding mmu-miR-17∼92 (PIG-17∼92), mutant miR-18a (PIG-Δ18a), miR-Ctrl, miR-18a, or mutant miR-18a mimic, as indicated. β-Actin was used as a loading control. The intensity of each band was measured with ImageJ software and labeled below the bands. **G:** Immunofluorescent staining shows localization of β-catenin protein in miR-Ctrl, miR-17∼92$^{Med}$, and miR-17∼92$^{Hi}$ cell lines. **H:** Expression of Wnt pathway—associated genes in miR-Ctrl, miR-17∼92$^{Med}$, and miR-17∼92$^{Hi}$ by real-time RT-PCR assay. Error bars represent ±SD (one-way analysis of variance in **A**, **D**, and **E** and Student's *t*-test in **H**). $*P < 0.05$, $**P < 0.01$. Original magnification, ×10 (with **boxed areas** in **top panels** enlarged in **bottom panels**; **G**).

were then treated with control Wnt3a; slides were next processed, as described previously, for tissue immunofluorescent staining.

## Clinical Specimens

Human gastric and colorectal specimens (primary and adjacent normal) were collected at the time of surgery. All samples were collected with informed consent of the patients, and the experiments were approved by the Institute Research Ethics Committee of Nanjing Medical University (Nanjing, Jiangsu, China).

## Statistical Analysis

Statistical significance was determined by the Student's *t*-test. Differences between individual groups were analyzed by one- or two-way analysis of variance test. Differences

were considered significant when $P < 0.05$ or $P < 0.01$, as indicated in the text.

## Results

### High Levels of miR-17∼92 Inhibit Tumor Growth and Metastasis *in Vivo*

Expression levels of miR-17∼92 in normal colon tissues were almost 50-fold higher than those in highly metastatic tumor tissues (Supplemental Figure S1A), whereas miR-17∼92 was 25-fold higher in higher-grade tumors when compared with highly carcinogenic low-grade tumors (Supplemental Figure S1B). This initial observation prompted us to further study the cellular and molecular mechanisms underlying the biological effect of varying levels of miR-17∼92 expression on colon tumor progression in animal models. First, we generated numerous monoclonals expressing different levels of the miR-17∼92 cluster in the CT26 colon cancer cell line by stably transfecting it with a control vector or PIG-miR-17∼92. Second, we randomly selected three monoclonals that represented expression levels of the miR-17∼92 cluster in human tumor tissue: a control vector transfected monoclonal, labeled miR-Ctrl; a stable low expression of the miR-17∼92 cluster (transfected with PIG-miR-17∼92, average fivefold higher than miR-Ctrl, and labeled miR-17∼92$^{Med}$); and a stable high expression of the miR-17∼92 cluster (transfected with PIG-miR-17∼92, average 50-fold higher than miR-Ctrl, labeled miR-17∼92$^{Hi}$). The expression levels of six individual mature miRNAs from the miR-17∼92 cluster were confirmed by quantitative real-time RT-PCR (Supplemental Figure S2A). We then compared the proliferation of all three cell lines that expressed different levels of the miR-17∼92 cluster. Unexpectedly, we found that there was no impact on colon cancer cell proliferation *in vitro* regardless of the levels of miR-17∼92 expression (Supplemental Figure S2B). Similarly, the expression levels of the miR-17∼92 cluster had no effect on cancer cell migration *in vitro* (Supplemental Figure S3A). To exclude the effect of cell type, we analyzed the effect of this cluster in two additional colon cancer cell lines (ie, CMT-93 and MCA38). As before, we did not observe any impact on the proliferation and migration of the cells (Supplemental Figures S2C and S3B), suggesting that the expression levels of miR-17∼92 did not modulate pathways associated with cell proliferation and migration *in vitro*.

We next asked whether expression levels of the miR-17∼92 cluster have an impact on tumor growth *in vivo* by s.c. injecting miR-Ctrl, miR-17∼92$^{Med}$, and miR-17∼92$^{Hi}$ cell lines into BALB/c mice. At 21 days after injection, we found that miR-17∼92$^{Hi}$ cells were almost completely eliminated; however, in contrast, we found that miR-17∼92$^{Med}$ cells were evident and proliferated at a faster rate than miR-17∼92$^{Hi}$ cells (Figure 1A). Next, to determine the biological effects of expression levels of miR-17∼92 on tumor metastasis *in vivo*, miR-Ctrl, miR-17∼92$^{Med}$, and miR-17∼92$^{Hi}$ were i.v. injected into immunocompetent mice. At 2 weeks after injection, livers and lungs were excised for immunofluorescence imaging. The liver and lung of mice injected with miR-17∼92$^{Hi}$ cells had no detectable signals; however, strong signals were detected in lung and liver from mice injected with miR-17∼92$^{Med}$ and miR-Ctrl compared with miR-17∼92$^{Hi}$ (Figure 1, B and C). Lungs were excised for further analysis. As expected, there were fewer metastases to lung in mice injected with miR-17∼92$^{Hi}$ cells, yet mice injected with miR-17∼92$^{Med}$ or miR-Ctrl had more metastases to the lung compared with miR-17∼92$^{Hi}$ (Figure 1D). To determine whether the results previously presented can be generalized, three additional clones from each transfected CT26 cell line were randomly selected and examined for their *in vitro* (Supplemental Figure S4A) and *in vivo* (Supplemental Figure S4, B and C) growth and metastasis. Results similar to those obtained in the original experiments were obtained from the additional three clones tested. To further demonstrate whether miR-17∼92$^{Hi}$ contributes to the prevention of tumor metastasis from the primary tumor to metastatic organs, the 4T1 breast tumor metastasis model was tested by injecting 4T1 tumor cells into mammary fat pads. The results suggest that higher levels of miR-17∼92, expressed in 4T1 tumor cells, prevent tumor growth and tumor lung metastasis (Supplemental Figure S5, A and B). Collectively, these results suggest that higher levels of miR-17∼92 inhibit tumor metastasis to lung and liver. Clinical evidence indicates that colon cancers have a greater potential for metastasis to the liver. To further address whether miR-17∼92 could inhibit colon cancer liver metastasis, we used a well-established liver metastasis model[36] (ie, splenic injection of tumor cells into immunocompetent mice). Surprisingly, there was no metastasis to liver in mice injected with miR-17∼92$^{Hi}$ cells, yet mice injected with miR-17∼92$^{Med}$ or miR-Ctrl had more metastases to the liver (Figure 1, E and F). Taken together, these data suggest that higher levels of miR-17∼92 are a critical step for suppressing both tumor cell growth and metastasis *in vivo*.

### Genome-Wide Prediction of Genes Targeted by Titrated Levels of miR-17∼92 Identifies β-Catenin Targeted by Higher Levels of miR-17∼92

To identify molecular mechanisms producing the different growth/metastasis patterns, we profiled gene expression in miR-Ctrl, miR-17∼92$^{Med}$, and miR-17∼92$^{Hi}$ cells using Affymetrix Murine GeneST Arrays. Whole-genome expression screening was performed with Affymetrix-Gene Chips after purification of total RNA from cloned miR-Ctrl, miR-17∼92$^{Med}$, and miR-17∼92$^{Hi}$ cells. The Ingenuity Pathway Analysis (Ingenuity Systems) of the mRNA arrays data [the raw data files are available from Supplemental Table S1 and the Gene Expression Omnibus database (*http://www.ncbi.nlm.nih.gov/geo*; accession number GSE55631)] led to the identification of several pathways regulated by miR-17∼92. Among those pathways affected by the expression levels of miR-17∼92, we noticed that the phosphatidylinositol 3-kinase (PI3K)/AKT pathway is one of the major pathways

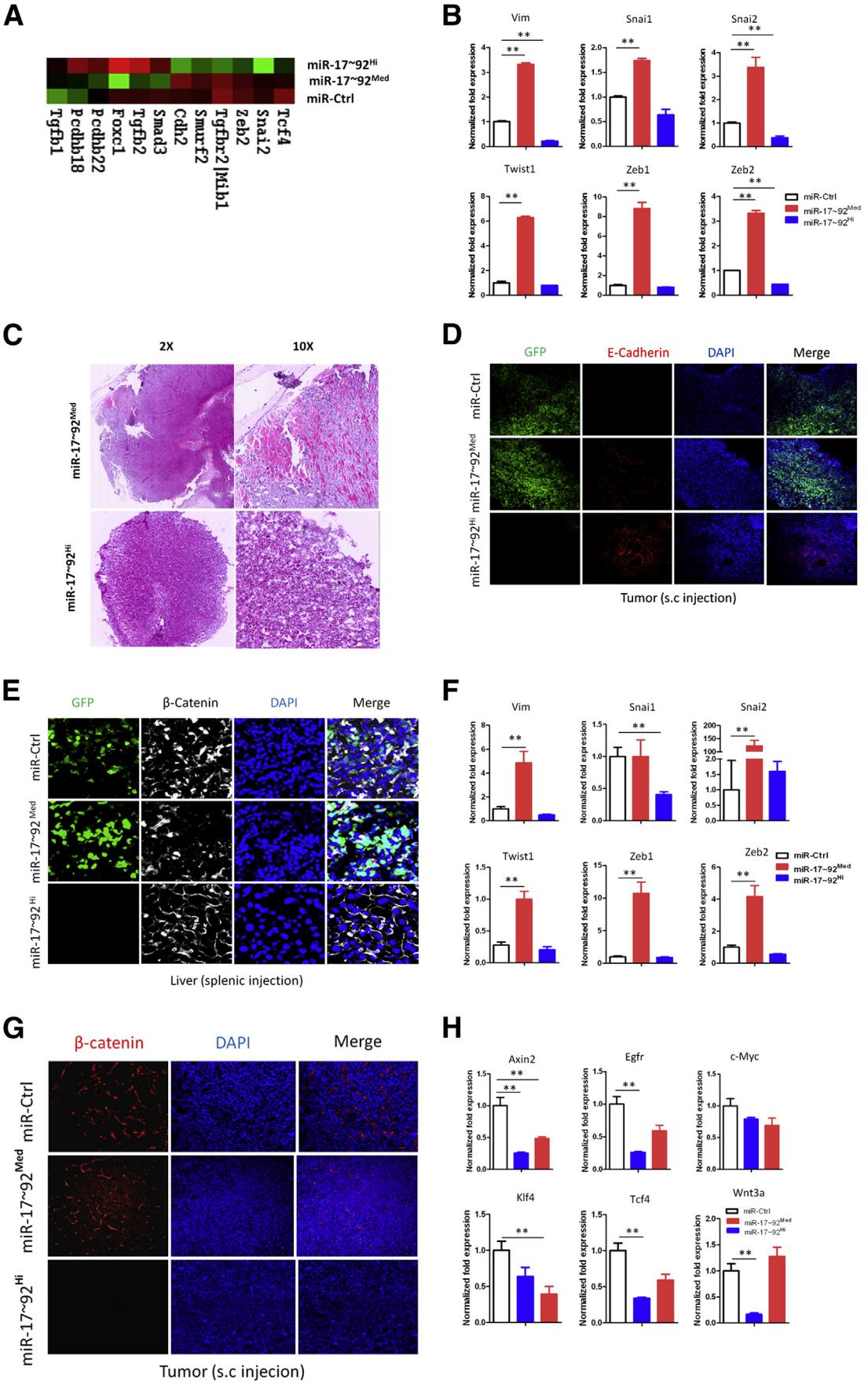
A
miR-17~92Hi
miR-17~92Med
miR-Ctrl
Tgfb1
Pcdhb18
Pcdhb22
Foxc1
Tgfb2
Smad3
Cdh2
Smurf2
Tgfbr2
Mib1
Zeb2
Snai2
Tcf4
B
Vim
Snai1
Snai2
Twist1
Zeb1
Zeb2
Normalized fold expression
miR-Ctrl
miR-17~92Med
miR-17~92Hi
C
2X
10X
miR-17~92Med
miR-17~92Hi
D
GFP
E-Cadherin
DAPI
Merge
miR-Ctrl
miR-17~92Med
miR-17~92Hi
Tumor (s.c injection)
E
GFP
β-Catenin
DAPI
Merge
miR-Ctrl
miR-17~92 Med
miR-17~92 Hi
Liver (splenic injection)
F
Vim
Snai1
Snai2
Twist1
Zeb1
Zeb2
Normalized fold expression
miR-Ctrl
miR-17~92Med
miR-17~92Hi
G
β-catenin
DAPI
Merge
miR-Ctrl
miR-17~92Med
miR-17~92Hi
Tumor (s.c injecion)
H
Axin2
Egfr
c-Myc
Klf4
Tcf4
Wnt3a
Normalized fold expression
miR-Ctrl
miR-17~92Med
miR-17~92Hi

regulated when medium levels of miR-17∼92 were expressed in CT26 cells (Supplemental Figure S6A). In contrast, when higher levels of miR-17∼92 were expressed, genes associated with colorectal cancer metastatic pathways were found to be involved (Supplemental Figure S6B). Most of the genes, such as *Wnt1*, *Wnt7b*, *Fzd6*, *Tcf4*, *Snai2*, and others identified in the colorectal cancer metastasis cluster, regulate the Wnt/β-catenin pathway (Supplemental Figure S6B). The Wnt/β-catenin pathway is well known to play a crucial role in colon cancer development.[37,38] The miR-17∼92 regulates the PI3K/AKT pathway through targeting *PTEN*; however, to our knowledge, no data are published suggesting that miR-17∼92 regulates the Wnt/β-catenin pathway.

By using public algorithms prediction analysis (TargetScan and RNABrid), we found that miR-17-92 targeted *Ctnnb1* (Figure 2A and Supplemental Figure S7A), which encodes β-catenin, which plays an important role in tumorigenicity through activation of the Wnt signaling pathway. These data led us to hypothesize that different levels of miR-17∼92 could shift it from an oncogene to a tumor suppressor through targeting different pathways: medium levels of miR-17∼92 might target *PTEN*, whereas higher levels of miR-17∼92 target the Wnt/β-catenin pathway. The data generated from luciferase reporter assays and Western blot analysis support the idea that medium levels of miR-17∼92 targeted *PTEN*, resulting in activation of the PI3K/AKT pathway, whereas higher levels of miR-17∼92 inhibited the Wnt/β-catenin pathway by targeting *Ctnnb1* (Figure 2, A–C). Although data from other laboratories[39,40] and ours (Supplemental Figure S7B) show that lower levels of miR-17∼92 down-regulate *PTEN*, there is no evidence that miR-17∼92 regulates expression of β-catenin. The results from the Topflash activity assay and Western blot analysis of all four cloned miR-Ctrl, miR-17∼92$^{Med}$, and miR-17∼92$^{Hi}$ cell lines further suggest that higher levels of miR-17∼92 suppress Wnt/β-catenin/TCF4 transcription activity through targeting β-catenin (Supplemental Figure S7C). To further identify which miRNAs in the miR-17∼92 cluster play a dominant role in targeting β-catenin genes, *Ctnnb1*-3′UTR expression vector was cotransfected with each mutant of miR-17∼92 (dela-miR-17/20a, dela-miR-18a, dela-miR-19a, and dela-miR-92a). The results from luciferase assays suggest that mutation of miR-18a significantly reverses the inhibitory effect of miR-17∼92 on the expression of β-catenin (Figure 2D). This was further confirmed by transfection of mutant miR-18a in which the β-catenin binding sites were mutated (Figure 2, E and F). We further analyzed the potential miR-17∼92 targeting sites within the *Ctnnb1* gene; we found miR-17∼92 target sequencing located in the coding sequence and 3′UTR. To exclude the possibility that miR-17∼92 might directly target the coding sequence, we cotransfected miR-17∼92 and β-catenin expression vector without 3′UTR (β-catenin-s33y). We found that miR-17∼92 did not inhibit mRNA expression of β-catenin (Supplemental Figure S7D).

Because translocation of β-catenin is the key step for activating the Wnt pathway–mediated activity of the TCF4 transcriptional machinery, we first analyzed the localization of β-catenin by immunofluorescence staining. As expected, there was significant reduction of both cytoplasmic and nuclear β-catenin levels in the miR-17∼92$^{Hi}$ cell line (Figure 2G). Next, to investigate whether the Wnt/β-catenin pathway transcriptional activity was affected by miR-17∼92, we performed the Topflash activity assay in the miR-Ctrl, miR-17∼92$^{Med}$, and miR-17∼92$^{Hi}$ cell lines. As expected, the Wnt transcriptional activity was dramatically reduced and could not be reversed by the Wnt/β-catenin activator, Wnt-3a (Supplemental Figure S7, E and F), suggesting that higher levels of miR-17∼92 repress canonical Wnt signaling downstream of the Wnt pathway, mainly by inhibiting β-catenin.

To address potential associations between miR-17∼92 levels and Wnt activity, we further examined the mRNA abundance of TCF4/LEF1 target genes. There was a significant decrease of multiple Wnt target genes downstream of β-catenin, including *Axin2*, *Ccnd1*, *E2f1*, *Klf4*, *Lef1*, and *Wnt3a* (Figure 2H). Taken together, these data demonstrated that medium levels of miR-17∼92 induce activation of the PI3K/AKT pathway by targeting *PTEN*, but higher levels of miR-17∼92 inhibit the Wnt/β-catenin pathway activity by targeting β-catenin.

## High Levels of miR-17∼92 Inhibit EMT by Targeting the Wnt/β-Catenin Pathway

The Wnt/β-catenin pathway has been known to contribute to therapeutic resistance and tumor metastasis by modulating epithelial-mesenchymal transition (EMT).[41,42] There was a dramatic increase of mesenchymal markers in the CT26 mouse tumor cell line with higher activity of the Wnt/β-catenin signaling pathway compared with the nontumorigenic

**Figure 3** Activation of Wnt/β-catenin pathway by miR-17∼92$^{Med}$ promotes tumor metastasis through inducing EMT. **A:** The heat map of EMT-associated genes targeted by miR-17∼92$^{Med}$ and miR-17∼92$^{Hi}$. **B:** Expression of EMT-associated genes in miR-Ctrl, miR-17∼92$^{Med}$, and miR-17∼92$^{Hi}$ by real-time RT-PCR assay. **C:** H&E staining of tumors from 14-day tumor-bearing mice injected s.c. with miR-17∼92$^{Med}$ and miR-17∼92$^{Hi}$ cell lines. **D:** Immunofluorescent staining shows the signal intensity of E-cadherin in the tumor of BALB/c mice injected s.c. with miR-Ctrl, miR-17∼92$^{Med}$, and miR-17∼92$^{Hi}$ tumor cells (GFP$^{+}$) on day 14 after injection. Tissues were counterstained with DAPI (blue). **E:** Immunofluorescent staining showing the intensity signal of β-catenin in the liver of BALB/c mice intrasplenically injected with miR-Ctrl, miR-17∼92$^{Med}$, or miR-17∼92$^{Hi}$ tumor cells (GFP$^{+}$) on day 14 after injection. Tissues were counterstained with DAPI (blue). **F:** Expression of EMT-associated genes in tumor cells recovered from miR-Ctrl, miR-17∼92$^{Med}$, or miR-17∼92$^{Hi}$ liver tumors by real-time RT-PCR assay. **G:** Immunofluorescent staining shows the signal intensity of β-catenin in the divided tumor tissues of BALB/c mice s.c. injected with miR-Ctrl, miR-17∼92$^{Med}$, or miR-17∼92$^{Hi}$ tumor cells on day 14 after injection. Tumor tissues were counterstained with DAPI (blue). **H:** Real-time RT-PCR assay quantification of the expression of Wnt-associated genes in tumor cells recovered from miR-Ctrl, miR-17∼92$^{Med}$, or miR-17∼92$^{Hi}$. Error bars represent ±SD (Student's *t*-test in **B** and **F** and two-way analysis of variance in **H**). $^{**}P < 0.01$. Original magnification, ×10 (**D**, **E**, and **G**).

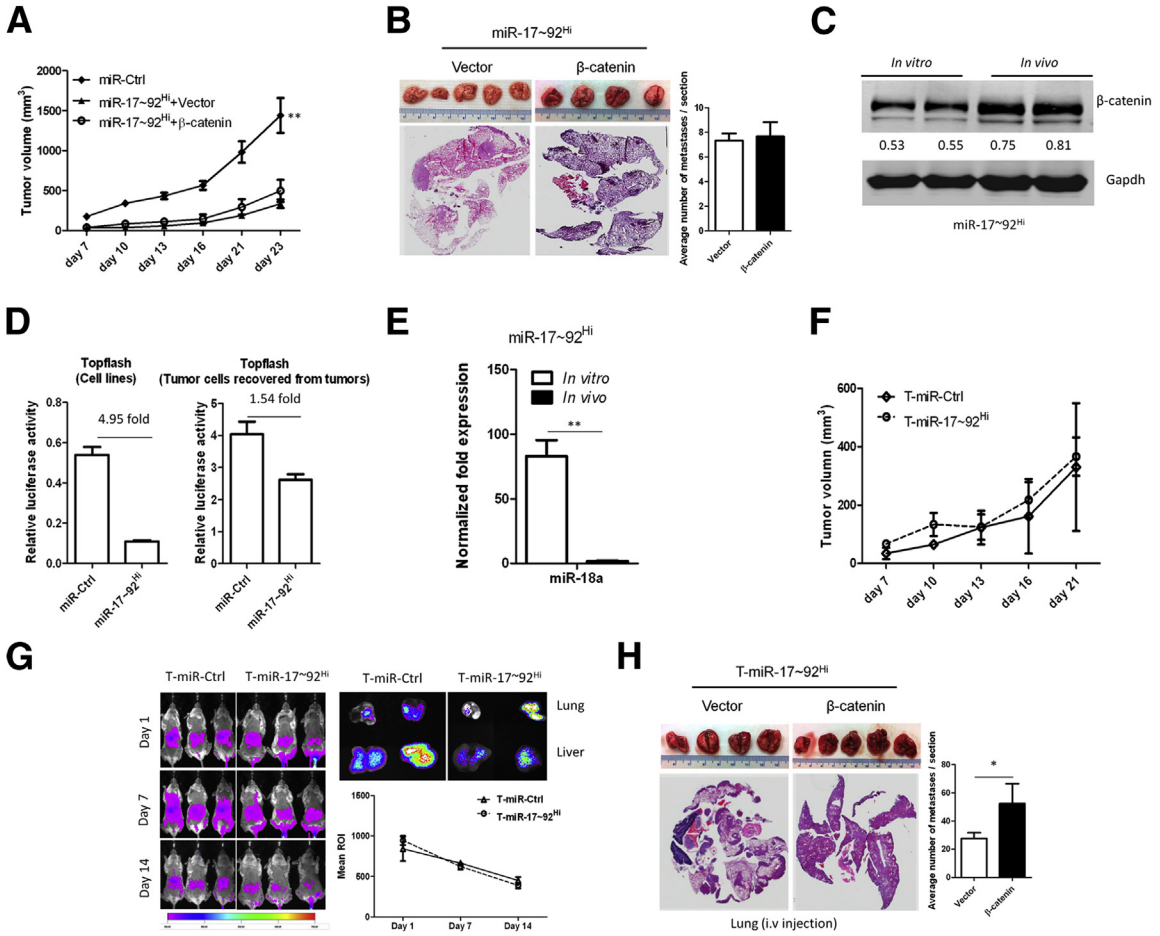


**Figure 4** High-level miR-18a in the context of the *miR-17∼92* cluster inhibits tumor progression through targeting β-catenin. **A:** Growth curve of miR-Ctrl and miR-17∼92$^{Hi}$ cell lines transfected with a control vector or MSCV-β-Catenin-ΔGSK-KT3 (β-catenin) in BALB/c mice (five mice per group). **B:** The morphological characteristics and H&E staining of lung tumors from 21-day tumor-bearing mice. Mice were injected i.v. with the miR-17∼92$^{Hi}$ cell line and transfected with a control vector or MSCV-β-Catenin-ΔGSK-KT3 (β-catenin). Histogram shows the number of metastatic sites per section. **C:** Western blot analysis shows the expression of the β-catenin protein in miR-17∼92$^{Hi}$ cells and tumor cells recovered from miR-17∼92$^{Hi}$ tumor-bearing mice at 21 days after s.c. injection into BALB/c mice. GAPDH was used as a loading control. **D:** Detection of Wnt/TCF4 activity in the miR-17∼92$^{Hi}$ cell line and tumor cells recovered from miR-17∼92$^{Hi}$ tumors at 21 days after s.c. injection into BALB/c mice using the Topflash luciferase assay. **E:** Quantification of the expression levels of miR-18a expressed in miR-17∼92$^{Hi}$ cell lines and tumor cells recovered from miR-17∼92$^{Hi}$ tumors at 21 days after s.c. injection into BALB/c mice by quantitative real-time RT-PCR. Error bars represent ±SD (Student's *t*-test). **F:** Growth curves of miR-Ctrl (T-miR-Ctrl) and miR-17∼92$^{Hi}$ (T-miR-17∼92$^{Hi}$) tumor cells recovered from tumors (14 days after s.c. injection of CT26/miR-Ctrl or CT26/miR-17∼92$^{Hi}$ monoclonal cells into BALB/c mice) in BALB/c mice (five mice per group; two-way analysis of variance). T-miR-Ctrl and T-miR-17∼92$^{Hi}$ tumor cells recovered from tumors (14 days after s.c. injection of CT26/miR-Ctrl or CT26/miR-17∼92$^{Hi}$ monoclonal cells into BALB/c mice) were labeled with DIR dye. DIR dye—labeled cells were then injected i.v. into 6-week-old female BALB/c mice. **G:** Tumor cell metastasis was monitored using a live imaging system by detecting the DIR fluorescence; a representative image from each group of tumor-bearing mice is shown. The signals of the DIR-labeled tumor cells in the lung and mean intensity of the DIR fluorescence at different time points. Mean intensity of region of interest = Sum Intensity/Area ($n = 5$). **H:** The morphological characteristics and H&E staining of lung tumors from 21-day tumor-bearing mice. Mice were injected i.v. with the T-miR-17∼92$^{Hi}$ cell line and transfected with a control vector or MSCV-β-Catenin-ΔGSK-KT3 (β-catenin). The histogram shows the number of metastases per section. Error bars represent ±SD (two-way analysis of variance in **A** and **G** and Student's *t*-test in **B**, **D**, **E**, and **H**). $^*P < 0.05$, $^{**}P < 0.01$.

epithelial cell line CMT-93 (Supplemental Figure S8, A and B). We asked whether medium levels of miR-17∼92, leading to promotion of tumor metastasis, might be correlated with induction of Wnt/β-catenin—mediated induction of EMT. First, we analyzed EMT-associated markers in both miR-Ctrl, miR-17∼92$^{Med}$, and miR-17∼92$^{Hi}$ cell lines by using whole-genome expression screening. As predicted, there was a significant increase of mesenchymal markers and transcriptional factors in the miR-17∼92$^{Med}$ cell line (Figure 3, A and B). Second, E-cadherin, which was an epithelial marker, was dramatically increased in the miR-17∼92$^{Hi}$ cell line with a concomitant low activity of the Wnt signaling pathway, accompanied by a significant decrease of EMT-associated transcriptional factors (Figure 3B and Supplemental Figure S8C). Among those transcriptional factors suppressed by miR-17∼92$^{Hi}$, Snai2 is one of the most down-regulated genes in the miR-17∼92$^{Hi}$ cell line. To determine whether overexpression of Snai2 could reverse the effect of miR17∼92 on the reduction of genes associated with EMT transcriptional factors, miR-17∼92$^{Hi}$ cells were transfected

with an Snai2 expression vector. The results generated from real-time PCR suggested that overexpression of Snai2 in the miR-17∼92$^{Hi}$ cells fails to reverse miR-17∼92–dependent inhibition of expression of EMT-associated transcriptional factors (Supplemental Figure S9, A and B).

We then asked whether slightly increased levels of miR-17∼92 expressed in tumor (in this case, an average fivefold higher than control cells) are correlated with induction of EMT *in vivo*. Indeed, we found that there were more invasive tumor cells with lower expression levels of E-cadherin in miR-17∼92$^{Med}$ tumor compared with miR-17∼92$^{Hi}$ tumor (Figure 3, C and D). Furthermore, significantly up-regulated EMT-related genes in miR-17∼92$^{Med}$ tumor cells isolated from liver metastases correlates with induction of β-catenin transcriptional activity (Figure 3, E and F). Next, we determined whether increasing levels of miR-17∼92 could inhibit tumor progression through targeting β-catenin. There was a dramatic decrease in the expression levels of β-catenin in miR-17∼92$^{Hi}$ tumors (Figure 3G), accompanied by a lower Wnt/β-catenin transcriptional activity when compared with miR-Ctrl and miR-17∼92$^{Med}$ tumors (Figure 3H). Collectively, medium levels of miR-17∼92 induce genes associated with Wnt/β-catenin–mediated EMT and thereby promote tumor metastasis, whereas high levels of miR-17∼92 inhibit EMT.

### Higher Levels of miR-18a Are Required for Targeting β-Catenin to Inhibit Colon Tumor Progression

To further address whether Wnt/β-catenin is a pathway directly targeted by higher levels of miR-17∼92, we overexpressed β-catenin in miR-17∼92$^{Hi}$ cells by transfecting the cells with a β-catenin expression vector. Unexpectedly, we found that, although the β-catenin gene was stably overexpressed in miR-17∼92$^{Hi}$ cells (Supplemental Figure S10A), the protein level of β-catenin was not increased (Supplemental Figure S10B). This result supports the fact that miR-17∼92$^{Hi}$ cells transfected with a β-catenin expression vector could not reverse the high-level miR-17∼92–mediated suppressive effect of tumor growth in BALB/c mice (Figure 4, A and B), suggesting that unidentified factor(s) regulated by a higher level of miR-17∼92 may also have an effect on production of β-catenin protein.

Because our data (Figure 2, D–F) indicate that miR-18a, but not other miRNAs in the context of the miR-17∼92 cluster, plays a dominant role in suppression of expression of β-catenin, we took a complementary approach to further address whether higher levels of miR-18a in the miR-17∼92 cluster suppress oncogenic β-catenin. We analyzed the expression levels of β-catenin in surviving tumor cells recovered from miR-17∼92$^{Hi}$ tumors. There was a dramatic increase in expression levels of β-catenin in surviving miR-17∼92$^{Hi}$ tumor cells recovered from tumors (Figure 4, C and D). The role of miR-18a in regulating β-catenin was further supported by the fact that the expression levels of miR-18a were reduced significantly in surviving tumor cells isolated from miR-17∼92$^{Hi}$ tumors when compared with the miR-17∼92$^{Hi}$ cell line (Figure 4E). When these surviving tumor cells were re-injected into mice, they grew and metastasized as fast as control cells (Figure 4, F and G). Therefore, these data strongly suggest that higher levels of miR-18a in tumor cells result in down-regulation of β-catenin and subsequent inactivation of the Wnt/β-catenin pathway. To further confirm the role of higher levels of miR-17∼92 in inhibition of tumor progression through targeting β-catenin, surviving tumor cells isolated from miR-17∼92$^{Hi}$ tumor were transfected with the β-catenin expression vector. The reason for using surviving tumor cells isolated from miR-17∼92$^{Hi}$ tumor is that these surviving tumor cells transitioned from miR-17∼92$^{Hi}$ β-catenin$^{low}$ to miR-17∼92$^{Med}$ β-catenin$^{high}$ tumor cells. Strikingly, overexpression of β-catenin in these tumor cells promoted tumor cell metastasis to the lung in BALB/c mice when compared with these tumor cells transfected with a control vector (Figure 4H). Collectively, these data suggest that the level of miR-17∼92 expressed in the tumor cells dictates the role of β-catenin in tumor growth and metastasis. Sufficiently high enough levels of miR-17∼92, expressed in the tumor cells, are required for suppressing the oncogenic role of β-catenin.

## Discussion

We demonstrated that the expression of higher levels of the miR-17∼92 cluster inhibit tumor growth and metastasis *in vivo*; however, lower levels of the miR-17∼92 cluster did not suppress the oncogenic role of the β-catenin, resulting in accelerating tumor growth and tumor colonization at distant sites. Therefore, our findings could potentially be used to develop therapeutic strategies that take advantage of inducing high levels of the miR-17∼92 cluster to inhibit tumor growth and metastasis.

The relationship between imbalanced subset miRNA expression within a given miRNA cluster, such as miR-17∼92, and cancer progression has been observed in various human-derived cancer cells and cancer patient samples.[43] Whether quantitatively controlling levels of miRNA of a given miRNA cluster has effects on the promotion or inhibition of tumor growth and metastasis has not been fully addressed. We pursued an alternative approach to study whether quantitative expression of miRNA determined the outcome. On the basis of the data we generated from established stable colon cell lines that closely represent human colon cancer tissue, we determined that quantitatively controlling expression levels of the miR-17∼92 cluster is a critical step for regulating/controlling colon tumor growth and metastasis. Higher expression levels of the miR-17∼92 cluster inhibit both colon tumor growth and metastasis.

Furthermore, our results imply that the number of copies of the miR-17∼92 cluster may be important for sufficient targeting of β-catenin. Consistent with our observation, previous studies have demonstrated that genes considered as

oncogenes or tumor suppressors could function in a dose-dependent manner.[44,45] Recent studies have shown that miRNAs and long noncoding RNAs [competing endogenous RNAs (ceRNAs)] compete with each other for binding to targeting mRNAs.[5,46–48] We speculate that unidentified specific ceRNAs may compete with miR-17∼92. At medium concentrations of miR-17∼92, the miR-17∼92 binding sites might be occupied mostly by specific ceRNAs; however, high levels of miR-17∼92 may have the capacity to outcompete for binding to functional targets.

Dysregulation of miRNAs has been reported in various human cancers.[8] Circumstantial evidence points to the potential involvement of several miRNAs in tumorigenesis. Most of these miRNAs might act as integral parts of the molecular architecture of oncogene and tumor-suppressor networks, such as the miR-17∼92 cluster. Studies have demonstrated that overexpression of the miR-17∼92 cluster could promote tumorigenesis[9,10] and tumor angiogenesis.[13] We describe, for the first time to our knowledge, that the higher levels of the miR-17∼92 cluster in colon cancer cells function as a tumor suppressor. The difference in our results compared with other studies is the result of the critical issue of overexpression in levels of the miR-17∼92 cluster. These studies show the role of the miR-17∼92 cluster in tumorigenesis[9,10] and tumor angiogenesis,[13] without measuring the levels of the miR-17∼92 cluster expressed. In contrast, our data show that the oncogenic role of β-catenin is demonstrated under medium, but not higher, levels of the miR-17∼92 cluster in tumor cells, further pointing to the importance of levels of expression of the miR-17∼92 cluster in modulating tumor progression. The fact that the quantity of miRNA is a critical factor for determining its preferential targeting has also been reported by another group.[49] We speculate that when the tumor microenviroment is regulated by the medium levels of miR-17∼92, there are optimal conditions for miR-17∼92 binding to the 3′-UTR of *PTEN*, but not of β-catenin, and oncogenic β-catenin is the outcome. Reduction of the abundance of specific ceRNAs binding to miR-17∼92 or up-regulation of miR-17∼92 to certain levels (a threshold) results in an altered tumor microenvironment, producing optimal conditions for miR-17∼92 binding to the 3′-UTR of β-catenin that is generated. The existence of this threshold that controls miRNA switching target genes has been reported.[49] Results in the present study provide the foundation for further identifying the threshold (fold increase of miR-17∼92) that leads to switching from PTEN to β-catenin and factors that regulate this switch. Such as a pair of tumor suppressor/oncogene, PTEN/β-catenin, additional groups of tumor suppressors and oncogenes may be regulated by the levels of miRNAs, such as miR-17∼92, as demonstrated herein.

In addition, given the known importance of β-catenin in many different pathological processes, our finding that miR-17∼92 targets β-catenin provides a foundation for possible targeted delivery of miR-17∼92 to tumor tissue for cancer therapy and other diseases associated with dysregulated β-catenin.

The expression levels of miR-17∼92 did not modulate pathways associated with colon tumor cell proliferation and migration *in vitro*, whereas *in vivo* higher levels of miR-17∼92 remarkably inhibit tumor progression; thus, we speculate that the tumor microenvironment may play a role in miR-17∼92–mediated tumor progression. It is conceivable that immune cells, in particular immune cells infiltrating a tumor, may play a role in causing this discrepancy in terms of tumor cell growth *in vitro* and *in vivo*. In addition, the Wnt/β-catenin pathway may not play an essential role in the proliferation of tumor cells in an *in vitro* culture environment. However, the Wnt/β-catenin may have a causative role in tumor growth by different mechanisms, such as activation of tumor β-catenin causing up-regulated secretion of Wnt ligands that are required for activation of β-catenin in stromal cells located in tumor tissue and further enhancement of activation of the Wnt/β-catenin pathway in tumor cells in an autocrine manner and promotion of tumor growth. This may be one of the reasons why there was no difference in the *in vitro* proliferation of tumor cells regardless of the levels of miR-17∼92 expressed; *in vivo*, the proliferation of tumor cells with high levels of miR-17∼92 expression was not promoted because a Wnt/β-catenin–enriched tumor microenvironment was lacking. Data published by other groups suggest that miR-17∼92 regulates osteogenesis[25] and cardiac[26] differentiation in *in vitro* models through interaction with the Wnt signaling pathway. Those data further support our findings that miR-17∼92 plays a critical role in regulating the activity of Wnt signaling. However, caution must be exercised when drawing a conclusion as to whether β-catenin is targeted by miR-17-92$^{Hi}$ because we observed that overexpression of the β-catenin gene in miR-17-92$^{Hi}$ cells did not lead to increasing β-catenin protein and to reversing miR-17-92$^{Hi}$–mediated inhibition of tumor progression. We speculate that higher levels of miR-17∼92 may also have an effect on the expression of unidentified factor(s) that regulate the production of the β-catenin protein. It is well known that regulation of gene expression includes a wide range of mechanisms that are used by cells to increase or decrease the production of protein. Virtually any step of gene expression can be modulated, from RNA processing to translational initiation to the post-translational modification of a protein. Our observation will open a new avenue for further studying the molecular pathway to determine how the levels of miR-17-92 regulate the production of Wnt/β-catenin. On the basis of published data, it is conceivable that high levels of PTEN are likely to have a synergistic role with high levels of miR-17-92$^{Hi}$ in terms of enhancing the suppressive effect on tumor growth. Our finding may provide a rationale for treating certain types of cancer by codelivering high levels of miR-17∼92 and PTEN.

In summary, we demonstrated that quantitatively controlling expression of miR-17∼92 could shift this cluster from promoting to inhibiting tumor progression. By using genome-wide screening, we identified a novel target of the miR-17∼92 cluster, β-catenin. miR-17∼92 at medium levels targets to the tumor-suppressor gene, *PTEN*; higher levels of the miR-17∼92 cluster switch from PTEN to

oncogenes, including β-catenin. This finding uncovers the molecular mechanism underlying miR-17∼92–mediated inhibition of tumor progression and opens up a new avenue for studying dose responses of miRNAs to specific phenotypes in cancer.

## Acknowledgments

We thank Dr. Andrea Ventura for providing pMSCV PIG, PIG-miR-17∼92 WT, PIG-miR-19a,b, ΔPIG-miR-17/20a, ΔPIG-miR-18a, ΔPIG-miR-19a,b, and ΔPIG-miR-92a; Dr. David Piwnica-Worms for Topflash; and Dr. Jerald Ainsworth for editorial assistance.

## Supplemental Data

Supplemental material for this article can be found at *http://dx.doi.org/10.1016/j.ajpath.2014.01.037*.

## References

1. Hutvagner G, McLachlan J, Pasquinelli AE, Balint E, Tuschl T, Zamore PD: A cellular function for the RNA-interference enzyme Dicer in the maturation of the let-7 small temporal RNA. Science 2001, 293:834–838
2. Han J, Lee Y, Yeom KH, Nam JW, Heo I, Rhee JK, Sohn SY, Cho Y, Zhang BT, Kim VN: Molecular basis for the recognition of primary microRNAs by the Drosha-DGCR8 complex. Cell 2006, 125:887–901
3. Lewis BP, Burge CB, Bartel DP: Conserved seed pairing, often flanked by adenosines, indicates that thousands of human genes are microRNA targets. Cell 2005, 120:15–20
4. Volinia S, Calin GA, Liu CG, Ambs S, Cimmino A, Petrocca F, Visone R, Iorio M, Roldo C, Ferracin M, Prueitt RL, Yanaihara N, Lanza G, Scarpa A, Vecchione A, Negrini M, Harris CC, Croce CM: A microRNA expression signature of human solid tumors defines cancer gene targets. Proc Natl Acad Sci U S A 2006, 103:2257–2261
5. Poliseno L, Salmena L, Zhang J, Carver B, Haveman WJ, Pandolfi PP: A coding-independent function of gene and pseudogene mRNAs regulates tumour biology. Nature 2010, 465:1033–1038
6. Yamamichi N, Shimomura R, Inada K, Sakurai K, Haraguchi T, Ozaki Y, Fujita S, Mizutani T, Furukawa C, Fujishiro M, Ichinose M, Shiogama K, Tsutsumi Y, Omata M, Iba H: Locked nucleic acid in situ hybridization analysis of miR-21 expression during colorectal cancer development. Clin Cancer Res 2009, 15:4009–4016
7. Wang P, Zou F, Zhang X, Li H, Dulak A, Tomko RJ Jr, Lazo JS, Wang Z, Zhang L, Yu J: microRNA-21 negatively regulates Cdc25A and cell cycle progression in colon cancer cells. Cancer Res 2009, 69:8157–8165
8. Lu J, Getz G, Miska EA, Alvarez-Saavedra E, Lamb J, Peck D, Sweet-Cordero A, Ebert BL, Mak RH, Ferrando AA, Downing JR, Jacks T, Horvitz HR, Golub TR: MicroRNA expression profiles classify human cancers. Nature 2005, 435:834–838
9. He L, Thomson JM, Hemann MT, Hernando-Monge E, Mu D, Goodson S, Powers S, Cordon-Cardo C, Lowe SW, Hannon GJ, Hammond SM: A microRNA polycistron as a potential human oncogene. Nature 2005, 435:828–833
10. Mu P, Han YC, Betel D, Yao E, Squatrito M, Ogrodowski P, de Stanchina E, D'Andrea A, Sander C, Ventura A: Genetic dissection of the miR-17∼92 cluster of microRNAs in Myc-induced B-cell lymphomas. Genes Dev 2009, 23:2806–2811
11. Olive V, Bennett MJ, Walker JC, Ma C, Jiang I, Cordon-Cardo C, Li QJ, Lowe SW, Hannon GJ, He L: miR-19 is a key oncogenic component of mir-17-92. Genes Dev 2009, 23:2839–2849
12. Yu Z, Wang C, Wang M, Li Z, Casimiro MC, Liu M, Wu K, Whittle J, Ju X, Hyslop T, McCue P, Pestell RG: A cyclin D1/microRNA 17/20 regulatory feedback loop in control of breast cancer cell proliferation. J Cell Biol 2008, 182:509–517
13. Dews M, Homayouni A, Yu D, Murphy D, Sevignani C, Wentzel E, Furth EE, Lee WM, Enders GH, Mendell JT, Thomas-Tikhonenko A: Augmentation of tumor angiogenesis by a Myc-activated microRNA cluster. Nat Genet 2006, 38:1060–1065
14. Yu Z, Willmarth NE, Zhou J, Katiyar S, Wang M, Liu Y, McCue PA, Quong AA, Lisanti MP, Pestell RG: microRNA 17/20 inhibits cellular invasion and tumor metastasis in breast cancer by heterotypic signaling. Proc Natl Acad Sci U S A 2010, 107:8231–8236
15. Eiriksdottir G, Johannesdottir G, Ingvarsson S, Björnsdottir IB, Jonasson JG, Agnarsson BA, Hallgrimsson J, Gudmundsson J, Egilsson V, Sigurdsson H, Barkardottir RB: Mapping loss of heterozygosity at chromosome 13q: loss at 13q12-q13 is associated with breast tumour progression and poor prognosis. Eur J Cancer 1998, 34:2076–2081
16. Stembalska A, Blin N, Ramsey D, Sasiadek MM: Three distinct regions of deletion on 13q in squamous cell carcinoma of the larynx. Oncol Rep 2006, 16:417–421
17. Zhang XL, Fu WL, Zhao HX, Zhou LX, Huang JF, Wang JH: Molecular studies of loss of heterozygosity in Chinese sporadic retinoblastoma patients. Clin Chim Acta 2005, 358:75–80
18. Lin YW, Sheu JC, Liu LY, Chen CH, Lee HS, Huang GT, Wang JT, Lee PH, Lu FJ: Loss of heterozygosity at chromosome 13q in hepatocellular carcinoma: identification of three independent regions. Eur J Cancer 1999, 35:1730–1734
19. Zhang L, Huang J, Yang N, Greshock J, Megraw MS, Giannakakis A, Liang S, Naylor TL, Barchetti A, Ward MR, Yao G, Medina A, O'Brien-Jenkins A, Katsaros D, Hatzigeorgiou A, Gimotty PA, Weber BL, Coukos G: microRNAs exhibit high frequency genomic alterations in human cancer. Proc Natl Acad Sci U S A 2006, 103:9136–9141
20. Clevers H: Wnt/beta-catenin signaling in development and disease. Cell 2006, 127:469–480
21. Jiang H, Xia J, Kang J, Ding Y, Wu W: Short hairpin RNA targeting beta-catenin suppresses cell proliferation and induces apoptosis in human gastric carcinoma cells. Scand J Gastroenterol 2009, 44:1452–1462
22. Maretto S, Cordenonsi M, Dupont S, Braghetta P, Broccoli V, Hassan AB, Volpin D, Bressan GM, Piccolo S: Mapping Wnt/beta-catenin signaling during mouse development and in colorectal tumors. Proc Natl Acad Sci U S A 2003, 100:3299–3304
23. Saydam O, Shen Y, Wurdinger T, Senol O, Boke E, James MF, Tannous BA, Stemmer-Rachamimov AO, Yi M, Stephens RM, Fraefel C, Gusella JF, Krichevsky AM, Breakefield XO: Downregulated microRNA-200a in meningiomas promotes tumor growth by reducing E-cadherin and activating the Wnt/beta-catenin signaling pathway. Mol Cell Biol 2009, 29:5923–5940
24. Ma L, Young J, Prabhala H, Pan E, Mestdagh P, Muth D, Teruya-Feldstein J, Reinhardt F, Onder TT, Valastyan S, Westermann F, Speleman F, Vandesompele J, Weinberg RA: miR-9, a MYC/MYCN-activated microRNA, regulates E-cadherin and cancer metastasis. Nat Cell Biol 2010, 12:247–256
25. Liu W, Liu Y, Guo T, Hu C, Luo H, Zhang L, Shi S, Cai T, Ding Y, Jin Y: TCF3, a novel positive regulator of osteogenesis, plays a crucial role in miR-17 modulating the diverse effect of canonical Wnt signaling in different microenvironments. Cell Death Dis 2013, 4:e539
26. Qin DN, Qian L, Hu DL, Yu ZB, Han SP, Zhu C, Wang X, Hu X: Effects of miR-19b overexpression on proliferation, differentiation, apoptosis and Wnt/beta-catenin signaling pathway in P19 cell model of cardiac differentiation in vitro. Cell Biochem Biophys 2013, 66:709–722
27. Veeman MT, Slusarski DC, Kaykas A, Louie SH, Moon RT: Zebrafish prickle, a modulator of noncanonical Wnt/Fz signaling, regulates gastrulation movements. Curr Biol 2003, 13:680–685
28. Guo W, Keckesova Z, Donaher JL, Shibue T, Tischler V, Reinhardt F, Itzkovitz S, Noske A, Zurrer-Hardi U, Bell G, Tam WL, Mani SA, van Oudenaarden A, Weinberg RA: Slug and Sox9 cooperatively determine the mammary stem cell state. Cell 2012, 148:1015–1028

29. Reya T, Duncan AW, Ailles L, Domen J, Scherer DC, Willert K, Hintz L, Nusse R, Weissman IL: A role for Wnt signalling in self-renewal of haematopoietic stem cells. Nature 2003, 423:409–414
30. Kolligs FT, Hu G, Dang CV, Fearon ER: Neoplastic transformation of RK3E by mutant beta-catenin requires deregulation of Tcf/Lef transcription but not activation of c-myc expression. Mol Cell Biol 1999, 19:5696–5706
31. O'Donnell KA, Wentzel EA, Zeller KI, Dang CV, Mendell JT: c-Myc-regulated microRNAs modulate E2F1 expression. Nature 2005, 435: 839–843
32. Bruns CJ, Liu W, Davis DW, Shaheen RM, McConkey DJ, Wilson MR, Bucana CD, Hicklin DJ, Ellis LM: Vascular endothelial growth factor is an in vivo survival factor for tumor endothelium in a murine model of colorectal carcinoma liver metastases. Cancer 2000, 89:488–499
33. Ilkovitch D, Lopez DM: The liver is a site for tumor-induced myeloid-derived suppressor cell accumulation and immunosuppression. Cancer Res 2009, 69:5514–5521
34. Xiang X, Zhuang X, Ju S, Zhang S, Jiang H, Mu J, Zhang L, Miller D, Grizzle W, Zhang HG: miR-155 promotes macroscopic tumor formation yet inhibits tumor dissemination from mammary fat pads to the lung by preventing EMT. Oncogene 2011, 30:3440–3453
35. Naik S, Piwnica-Worms D: Real-time imaging of beta-catenin dynamics in cells and living mice. Proc Natl Acad Sci U S A 2007, 104: 17465–17470
36. Kitakata H, Nemoto-Sasaki Y, Takahashi Y, Kondo T, Mai M, Mukaida N: Essential roles of tumor necrosis factor receptor p55 in liver metastasis of intrasplenic administration of colon 26 cells. Cancer Res 2002, 62:6682–6687
37. Suzuki H, Watkins DN, Jair KW, Schuebel KE, Markowitz SD, Chen WD, Pretlow TP, Yang B, Akiyama Y, Van Engeland M, Toyota M, Tokino T, Hinoda Y, Imai K, Herman JG, Baylin SB: Epigenetic inactivation of SFRP genes allows constitutive WNT signaling in colorectal cancer. Nat Genet 2004, 36:417–422
38. Vermeulen L, De Sousa EMF, van der Heijden M, Cameron K, de Jong JH, Borovski T, Tuynman JB, Todaro M, Merz C, Rodermond H, Sprick MR, Kemper K, Richel DJ, Stassi G, Medema JP: Wnt activity defines colon cancer stem cells and is regulated by the microenvironment. Nat Cell Biol 2010, 12:468–476
39. Wang F, Li T, Zhang B, Li H, Wu Q, Yang L, Nie Y, Wu K, Shi Y, Fan D: MicroRNA-19a/b regulates multidrug resistance in human gastric cancer cells by targeting PTEN. Biochem Biophys Res Commun 2013, 434:688–694
40. Xiao C, Srinivasan L, Calado DP, Patterson HC, Zhang B, Wang J, Henderson JM, Kutok JL, Rajewsky K: Lymphoproliferative disease and autoimmunity in mice with increased miR-17-92 expression in lymphocytes. Nat Immunol 2008, 9:405–414
41. Cai J, Guan H, Fang L, Yang Y, Zhu X, Yuan J, Wu J, Li M: MicroRNA-374a activates Wnt/beta-catenin signaling to promote breast cancer metastasis. J Clin Invest 2013, 123:566–579
42. Wu ZQ, Li XY, Hu CY, Ford M, Kleer CG, Weiss SJ: Canonical Wnt signaling regulates Slug activity and links epithelial-mesenchymal transition with epigenetic Breast Cancer 1, Early Onset (BRCA1) repression. Proc Natl Acad Sci U S A 2012, 109:16654–16659
43. Yanaihara N, Caplen N, Bowman E, Seike M, Kumamoto K, Yi M, Stephens RM, Okamoto A, Yokota J, Tanaka T, Calin GA, Liu CG, Croce CM, Harris CC: Unique microRNA molecular profiles in lung cancer diagnosis and prognosis. Cancer Cell 2006, 9:189–198
44. Sarkisian CJ, Keister BA, Stairs DB, Boxer RB, Moody SE, Chodosh LA: Dose-dependent oncogene-induced senescence in vivo and its evasion during mammary tumorigenesis. Nat Cell Biol 2007, 9: 493–505
45. Garcia-Cao I, Song MS, Hobbs RM, Laurent G, Giorgi C, de Boer VC, Anastasiou D, Ito K, Sasaki AT, Rameh L, Carracedo A, Vander Heiden MG, Cantley LC, Pinton P, Haigis MC, Pandolfi PP: Systemic elevation of PTEN induces a tumor-suppressive metabolic state. Cell 2012, 149:49–62
46. Seitz H: Redefining microRNA targets. Curr Biol 2009, 19:870–873
47. Karreth FA, Tay Y, Perna D, Ala U, Tan SM, Rust AG, DeNicola G, Webster KA, Weiss D, Perez-Mancera PA, Krauthammer M, Halaban R, Provero P, Adams DJ, Tuveson DA, Pandolfi PP: In vivo identification of tumor-suppressive PTEN ceRNAs in an oncogenic BRAF-induced mouse model of melanoma. Cell 2011, 147:382–395
48. Tay Y, Kats L, Salmena L, Weiss D, Tan SM, Ala U, Karreth F, Poliseno L, Provero P, Di Cunto F, Lieberman J, Rigoutsos I, Pandolfi PP: Coding-independent regulation of the tumor suppressor PTEN by competing endogenous mRNAs. Cell 2011, 147:344–357
49. Mukherji S, Ebert MS, Zheng GX, Tsang JS, Sharp PA, van Oudenaarden A: MicroRNAs can generate thresholds in target gene expression. Nat Genet 2011, 43:854–859